Environmental Modelling & Software 84 (2016) 349–362

Contents lists available at ScienceDirect

Environmental Modelling & Software

journal homepage: www.elsevier.com/locate/envsoft

# Modeling the potential effects of sea-level rise on the coast of New York: Integrating mechanistic accretion and stochastic uncertainty

Jonathan Clough*, Amy Polaczyk, Marco Propato

*Warren Pinnacle Consulting, Inc., PO Box 315, Waitsfield, VT 05673, USA*

ARTICLE INFO

*Article history:*
Received 18 January 2016
Received in revised form
4 May 2016
Accepted 27 June 2016
Available online 21 July 2016

*Keywords:*
Sea-level rise
Accretion
Uncertainty
SLAMM
New York

ABSTRACT

The Sea-Level Affecting Marshes Model was applied to coastal New York State at a 5 m horizontal resolution to investigate marsh conservation and potential migration under multiple sea-level rise scenarios. Feedbacks between sea-level rise and marsh accretion rates based on mechanistic modeling were included. Simulation results predict extensive marsh losses in microtidal regimes behind the barrier islands of Long Island, vulnerable dry lands on barrier islands, and opportunities for upland migration of coastal marshes. Results also indicate changes in the composition of marsh types. Confidence of predictions due to model parameter variabilities and spatial data error were estimated with the uncertainty estimation module. Likelihood maps of land cover changes were produced. Uncertainty results suggest that variability in land cover projections is mostly due to the wide range in potential sea-level rise signals by 2100 while impact from uncertainties in model parameters, spatial data errors and linked models is less significant.



## Software availability

> The SLAMM model used to produce these model runs is open source; version 6.2 is available at the following URL: http://warrenpinnacle.com/prof/SLAMM6.

## 1. Introduction

Tidal wetlands, located at the interface between land and tidal waters, are among the most susceptible ecosystems to accelerated sea-level rise (SLR). However, the relationship between tidal marshes and ocean levels is a complex one, incorporating several dynamic factors. Variables such as elevation of marshes relative to tides, frequency of wetland inundation, pore-water salinity, marsh biomass, subsidence, marsh substrate, and the settling of suspended sediment can all affect marsh responses to changing water levels. Furthermore, the migration of tidal wetlands inland in response to rising oceans can be affected by hydraulic connectivity, as well as the hard barriers of existing seawalls and development.

To assist land-use planners in identifying appropriate adaption strategies in response to potential impacts of SLR on tidal marshes and nearby areas in New York State (NYS), the New York State Energy Research and Development Authority (NYSERDA) funded a high resolution application of the Sea-Level Affecting Marshes Model (SLAMM) to the majority of the NYS coast (Fig. 1).

Based on a relatively simple framework, SLAMM simulates the dominant processes involved in wetland conversions and shoreline modifications during long-term sea level rise and uses a complex decision tree incorporating geometric and qualitative relationships to represent habitat changes (Clough et al., 2012). The SLAMM model will predict both the capability of existing salt marshes to survive an increase of sea level by maintaining elevation, and the colonization of marsh into areas previously high and dry as sea level increases. Predictions of wetland coverage are produced over decadal time steps assuming that at each time step marshes and wetlands can come to equilibrium with future water levels. The model has been under development since the mid-1980s (Park et al., 1989) and has been widely applied to assess wetland fate in the coastal United States (Craft et al., 2008; Galbraith et al., 2002; Lee et al., 1992, 1991; Park et al., 1991). The validity of the model has been recently tested with retrospective analyses in Florida (Geselbracht et al., 2011) and Louisiana (Glick et al., 2013). In Florida, the model was used to assess coastal forest loss when

* Corresponding author.
*E-mail addresses:* jclough@warrenpinnacle.com (J. Clough), apolaczyk@warrenpinnacle.com (A. Polaczyk), mpropato@warrenpinnacle.com (M. Propato).

http://dx.doi.org/10.1016/j.envsoft.2016.06.023
1364-8152/

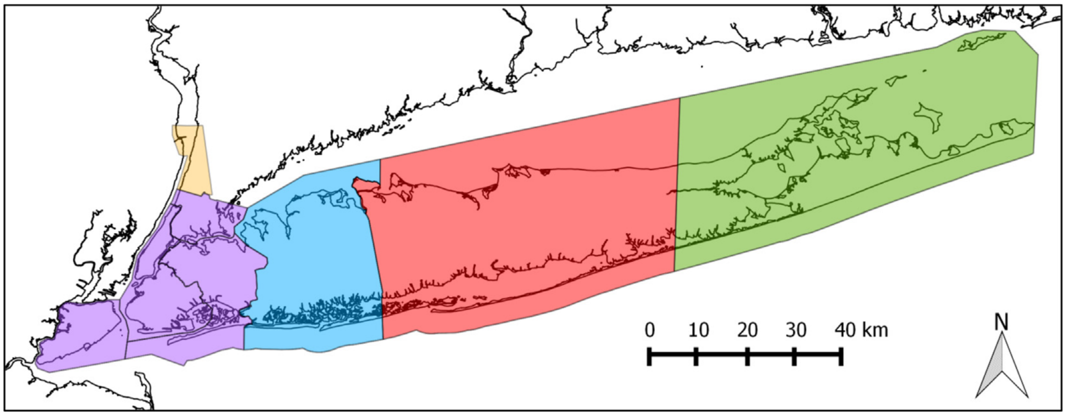


**Fig. 1.** Project study area as broken into five individual SLAMM projects.

compared to 30 years of field data. The authors concluded "overall, the model showed the same pattern of coastal forest loss as observed. In Louisiana, model calibration was conducted using a 1956–2007 observation period. Despite extremely limited historical data to initialize the model, hindcasting results predicted 35% total marsh loss versus observed 39%. Additional model testing was completed via a global sensitivity and uncertainty analysis to clarify the relationship between model input factors and output uncertainty (Chu-Agor et al., 2010). The SLAMM model was recently favorably evaluated using neutral models for the lower Pascagoula River basin, Mississippi (Wu et al., 2015). Mcleod et al. (2010) reviewed the model among a suite of sea-level rise impact models and stated "… the SLAMM model provides useful, high-resolution, insights regarding how sea-level rise may impact coastal habitats"

The main objective of this manuscript is to present and discuss the application of SLAMM to the New York coast. Although the base analysis considers a range of different possible SLR scenarios, the effects of various sources of uncertainties such as input parameters and driving data are not accounted for. In addition, refined and site-specific data are often not available requiring the use of regional data collected from literature and professional judgement in order to run the model. To ignore the effects of these uncertainties on predictions may make interpretation of the results and subsequent decision making misleading since the likelihood and probabilities of predicted outcomes would be unknown. A unique capability of the current version of SLAMM is the ability to aggregate multiple types of input-data uncertainty to create outputs accompanied by probability statements and confidence intervals. Uncertainty in elevation data layers have been considered by several modeling groups to various extents (Gesch, 2009; Gilmer and Ferdaña, 2012; Schmid et al., 2014). However, to the best of our knowledge, no other marsh migration model simultaneously accounts for the combined effects of uncertainty in spatial inputs (DEM, VDATUM, etc.) and parameter choices (accretion rates, tide ranges, etc.) on landcover projections. This added feature of SLAMM allows results to be evaluated in terms of their likelihood of occurrence with respect to input-data and parameter uncertainties. Further, by assigning wide ranges of uncertainty when appropriate, it permits the production of meaningful projections in areas where high-quality local data are not available.

## 2. Materials and methods

This section summarizes the data sources and the steps undertaken to build SLAMM models for the study area. However, for a more extensive and complete description, the reader can access the final project report at http://tinyurl.com/NYSERDASLAMM.

**Study Area.** Fig. 1 shows the entire study area which comprises all coastal regions of Long Island, New York City (NYC) and the Hudson River up to the Tappan Zee Bridge. The inland extent of the study area included all lands with elevations less than 5 m above mean tide level (MTL), except for NYC where the entire area was considered. The 5 m boundary elevation was selected to limit the study area to regions that could be affected by increased sea level under all the SLR scenarios considered (the maximum SLR examined was approximately 1.7 m by 2100).

### 2.1. Land cover data

Several data sources were used to characterize land cover types:

- *Nassau and Suffolk Counties*. For both the north and south shores of this study area, land cover information was derived from a 2004 National Wetlands Inventory (NWI) published by the U.S. Fish and Wildlife Service (http://www.fws.gov/wetlands/).
- *New York City*. The primary layer was provided by the New York State Department of Environmental Conservation (NYSDEC) dated 1999. To better reflect current land coverage, recent data provided by the NYC Department of Parks and Recreation (NYCDPR) were used to remove or add wetland areas. Land cover for Jamaica Bay, NY was derived from a 2008 high-resolution data. Finally, NWI data were also used for fresh water wetlands and to classify areas not well identified by the other data sources. Following extensive feedback and review from NYCDPR, all of these data sources were combined to create the final land cover layer for NYC.
- *Hudson River*. Land cover for this area was from 2007 data from the NYSDEC Hudson River Estuary Program.

The preparation of land-cover layers required several steps including conversion from the native land-cover classification to SLAMM categories, conversion to the project-specific GIS projection, overlaying of several data layers in order of their priorities, and conversion to raster maps of 5 m cell resolution.

Native wetland classifications for the different data sources were converted to SLAMM wetland categories with the assistance of NYC Parks and NYSDEC experts and using the conversion table from NWI categories to SLAMM that has been carefully vetted by Bill Wilen of NWI (Clough et al., 2012, Table 4).

The demarcation between developed and undeveloped dry land was determined based on a high-resolution impervious-surface data set created by the University of Vermont Spatial Analysis Lab using 2011 imagery obtained from the National Agricultural Imagery Program and for NYC a 2010 sub-meter resolution land cover dataset.

The total area studied amounts to over 580,000 ha, of which 210,292 ha are currently covered by dryland, 11,560 ha by tidal marshes, 5100 ha by beaches and tidal flat, 4100 ha of non-tidal marsh and the rest is open water.

Table 1 summarizes all land cover-types for the entire study area.

### 2.2. Elevation data

Original LiDAR data sets were 2011–2012 Coastal New York State LiDAR (Tidal Water Raster DEM), New York 2010 Lidar Coverage, USACE National Coastal Mapping Program, and 2012 USACE Post-Sandy LiDAR: NJ &NY. These recent LiDAR data all have a native resolution of 1 m, horizontal precisions ranging from 30 to 75 cm, and vertical precisions that range from 5 to 12 cm.

Starting from these LiDAR data, hydro-enforced Digital Elevation Model (DEM) maps were created for the entire study area. Hydrologic enforcement is performed to eliminate the effects of artificially raised topography (e.g. bridge elevations initially contained in the DEM or a missing culvert) that would otherwise block hydrologic flows. For this study, the New York State Accident Location Information System road centerline file and the National Hydrography Dataset were intersected to identify all culvert/bridge locations in the initial DEM that needed hydrologic enforcement.

In addition to the elevation layer a slope layer was created. The slope in degrees of each cell is a SLAMM model input and provides a range of elevations that can be observed in a cell. This information is used to calculate partial cell conversion. Slope rasters were derived from the hydro-enforced DEMs created above using the "slope tool" in ESRI's spatial analyst.

The NOAA VDATUM modeling product (National Ocean Service, 2013) was used to convert elevation data from NAVD88 to MTL, the vertical datum used by SLAMM.

### 2.3. Dikes and impoundments

Dike rasters were created using NWI data which provide a "diked or impounded" attribute for wetland areas only. These lands were assumed to be permanently protected from flooding. This procedure has the potential to miss dry lands that are protected by dikes and seawalls, however no additional diked areas in the study area were found when examining the US Army Corps of Engineers National Levee Database.

La Guardia Airport was assumed to be permanently protected by existing and future seawalls. In fact, without this assumption and with the available elevation data for the area, SLAMM would predict regular inundation from the east side of the airport. While La Guardia airport has occasionally been flooded in the past, currently-existing seawalls are not effectively represented in the DEM. In addition, there is an ongoing engineering project to improve airport protection against inundation.

### 2.4. SLR scenarios

Deterministic SLAMM simulations were produced under four scenarios of future SLR corresponding to the General Climate Model Maximum (GCM Max), 1 m by 2100, and the Rapid Ice Melt Minimum and Maximum (RIM Min and RIM Max) scenarios as described in the New York State ClimAID Report (2011) ranging from SLR increases of 71.9–172.2 cm (28.3–67.8 inches) by 2100 (Fig. 2).

The SLR scenarios shown in Fig. 2 above are "relative" sea-level rise estimates—they are specific to the study area as they include local subsidence. Therefore, SLAMM scenarios do not need to be corrected for differences between local (or relative) SLR and global (or eustatic) SLR trends. According to NOAA, historic sea-level rise trends along the New York coast range from 2.35 mm/yr at Kings Point to 2.78 mm/yr in Montauk. Therefore each of the four scenarios simulated represents a significant acceleration of SLR from the historical trend.

### 2.5. Tidal and inundation data

Tide-range data were collected from NOAA tidal datums and 2011 tide prediction tables (National Ocean Service, 2010) within the study area. An additional tide data source was the LIShore historical tide database (Wilson, 2013). Overall, 233 data sources distributed throughout the study area were used to model the spatially different tidal regimes (detailed location and values can be found in the Appendix B of the project report).

To determine the elevation at the wetland-to-dryland boundary, NOAA historical inundation data were evaluated. By analyzing the local relationship between frequency of inundation, elevations and current land cover, the elevation that differentiates coastal wetlands and dry lands is approximately the height inundated once every 30 days, which is in agreement with previous model applications (e.g. Geselbracht et al., 2011; Table 1, footnote f). A linear relationship between the 30 day inundation level and the great diurnal tide range was determined in order to assess dry to wet land boundaries in all study areas.

### 2.6. Tidal marsh accretion rates

A key feature of this SLAMM application is the accounting for what are potentially critical feedbacks between tidal-marsh accretion rates and SLR (Kirwan et al., 2010). In tidal marshes, increasing inundation can lead to additional deposition of inorganic sediment that can help tidal wetlands keep pace with rising sea levels (Reed, 1995). In addition, salt marshes will often grow more rapidly at lower elevations allowing for further inorganic sediment trapping (Morris et al., 2002). Therefore, as water levels rise due to SLR, to some extent marshes can move vertically to maintain their location in the tidal frame.

Feedback relationships were investigated using observed accretion rates as compared to marsh platform elevations. When not reported in the data source, marsh platform elevations were estimated from the site DEM using the coordinates provided in the citations. There is significant uncertainty in terms of assigning elevations to these marsh platforms, especially when core data (Pb210 measurements) were used to derive accretion rates. A more detailed discussion about this is provided in the uncertainty estimation section below.

Accretion curves were derived for the SLAMM categories of regularly-flooded marsh (RFM) and irregularly-flooded marsh (IFM). Qualitatively, RFM includes low to mid marshes, while IFM includes high marshes.

- **IFM Accretion.** Data from 15 different sites were evaluated (Armentano and Woodwell, 1975; Cochran et al., 1998; Flessa et al., 1977; Kolker, 2005; Maher, 2013). Accretion rates for high marshes ranged from 2.1 to 7.9 mm/year. No strong relationship between accretion rates and derived elevations for these sites was evident, nor was there any spatial trend within the study area. This may be expected as IFM are subject to less-frequent flooding than lower marshes, and therefore less sedimentation. Based on the data analysis, IFM accretion rate was set to the average value of the available data with a very mild linear

**Table 1**
Initial-Condition Land cover categories for entire New York study area.

| Land cover type | Area (ha) | % |
|---|---|---|
| Estuarine Open Water | 194,333 | 33.4 |
| Open Ocean | 153,469 | 26.4 |
| Undeveloped Dry Land | 127,226 | 21.9 |
| Developed Dry Land | 83,065 | 14.3 |
| Irreg.-Flooded Marsh | 9119 | 1.6 |
| Swamp | 3466 | 0.6 |
| Inland Open Water | 2877 | 0.5 |
| Regularly-Flooded Marsh | 1609 | 0.3 |
| Ocean Beach | 1877 | 0.3 |
| Estuarine Beach | 1868 | 0.3 |
| Tidal Flat | 1394 | 0.2 |
| Trans. Salt Marsh | 420 | 0.1 |
| Inland-Fresh Marsh | 639 | 0.1 |
| Tidal Swamp | 335 | 0.1 |
| Tidal-Fresh Marsh | 78 | <0.1 |
| Inland Shore | 35 | <0.1 |
| Rocky Intertidal | 25 | <0.1 |
| Riverine Tidal | 6 | <0.1 |
| Ocean Flat | <1 | <0.1 |
| **Total (incl. water)** | **581,843** | 100 |

feedback, ranging from 4.06 mm/year at the highest elevation to 4.23 mm/year at the lower end of the elevation range of this marsh type. The high degree of uncertainty of these data is accounted for and discussed in the uncertainty estimation section.

- **RFM Accretion.** To properly account for feedbacks in regularly-flooded marshes, version 3.4 of the Marsh Equilibrium Model, (MEM) developed by Dr. Morris and coworkers at the University of South Carolina (Hagen et al., 2012; Morris et al., 2002), was calibrated to site-specific data for regularly-flooded salt marshes. MEM is mechanistic model that accounts for the physical and biological processes that determine the resiliency of salt marshes to accelerations in sea-level rise. Use of a mechanistic model such as MEM can have several benefits over an empirical curve fitting. First, MEM can estimate marsh accretion-rates at elevations low in the tidal frame where marshes do not exist today but where marshes could fall to in the future as a result of increased SLR. Second, results from this model can be extrapolated to geographic areas where there are no accretion data available, but other physical/biological parameters *are* available (e.g. suspended sediment concentrations or tidal regimes).

MEM includes several key physical and biological input parameters. Some of them are usually readily available (e.g. tide ranges, suspended sediment concentration, initial sea-level and marsh platform elevation), while other are uncertain or site specific (e.g. sediment trapping coefficient, or below-ground turnover rate). The approach taken was to estimate MEM input parameters based on observations when available and fit a small set of uncertain model parameters using observed accretion rates in the area. Available data were spatially separated into North of Long Island, South of Long Island, and the Peconic Bay System due to differences in tide-ranges, salinity, and suspended-sediment concentrations.

- Accretion data from 13 sites were evaluated (Cochran et al., 1998; Kolker, 2005; Maher, 2013) and ranged from 1.4 to 7.0 mm/year.
- Suspended sediment data (in the form of total suspended solids or TSS) were collected from the US EPA STORET Data Warehouse, The City of New York Department of Environmental Protection, and the Peconic Estuary Program and varied between from 8.2 mg/L in NY Harbor and Staten Island to 20 mg/L in the Hudson River study area. These last data, although relatively high compared to other portions of the study area, were however at the low end of the 20–40 mg/L range for the majority of the Hudson River Estuary described by Woodruff et al. (2001).
- Marsh biomass data were limited. Values between 700 and 1000 g/m2 have been measured at Hoadley, Jarvis and Sherwood marshes in CT (Anisfeld, 2014). Based on these observations, the North Shore of the Long Island was calibrated using an optimal peak biomass of 800 g/m2. Hartig and coworkers measured biomass of *Spartina alterniflora* ranging from 700 to 1450 g/m2 in Jamaica Bay (Hartig et al., 2002). The value of 1150 g/m2 was used as optimal peak biomass for the MEM describing accretion rates in the South Shore of Long Island. For the Peconic Bay system, the highest measured accretion rates were observed. To match these rates within the MEM model, a higher biomass of 2000 g/m2 was used in this region. It is presumed that higher marsh biomass in this region is due to

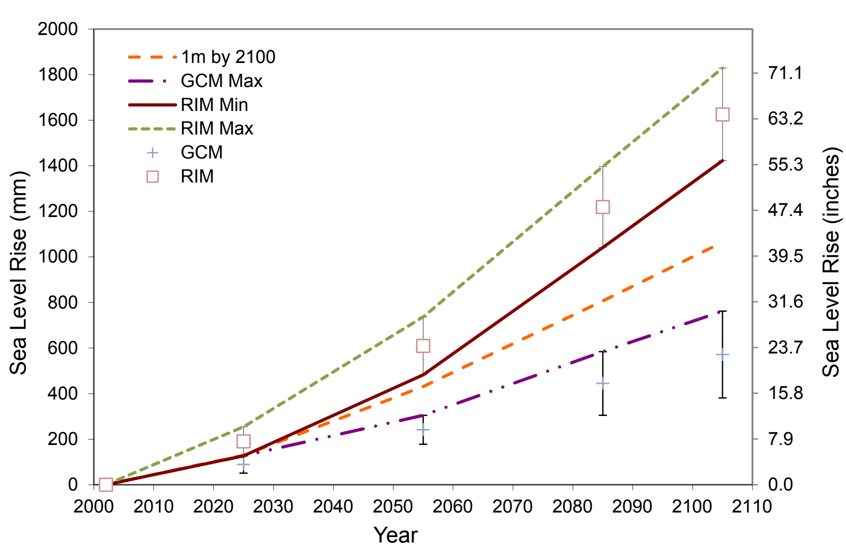


**Fig. 2.** Sea-level rise scenarios simulated using SLAMM compared to the NYS ClimAID General Climate Model (GCM) and Rapid Ice Melt (RIM) model predictions.

lower observed salinity (15.8 PSU in this region vs. 26–28 PSU in the north and south shores of Long Island, Pierson, 2013). Recent studies on low salinity marshes (Schile et al., 2014) measured average peak biomass ranging from 1600 to 2400 g/m2 while multiple studies indicate that the aboveground growth rate of *S. alterniflora* is reduced as salinity increases (Dame and Kenny, 1986; Haines and Dunn, 1976; Linthurst and Blum, 1981; Linthurst and Seneca, 1981; Mendelssohn and Marcellus, 1976; Zedler, 1980) and that this results in lower aboveground biomass (Vasquez et al., 2006).

The best-fit MEM curves were identified the web version of MEM (http://129.252.139.114/model/marsh/mem2.asp). A third-order polynomial fit of these curves was then implemented into SLAMM. The resulting curves used in SLAMM are illustrated in Fig. 4. These relationships were translated into polynomial curves and fed directly into the SLAMM model to describe response of various marshes when subjected to different flooding frequencies.

For Staten Island and the Hudson River where no accretion data are available, the calibrated MEM models for the South Shore of Long Island and the Peconic Bays were extrapolated by incorporating known TSS and tide-range information for these areas but keeping all other input parameters unchanged. The Staten Island prediction is essentially identical to the derived model for Long Island South. However, due to the high TSS in the Hudson River, low marshes in that area are predicted to have accretion rates as high as 11 mm/year. Since low marshes currently occupy a minimal portion of the Hudson River study area, this high accretion value may play a significant role only under the most aggressive SLR scenarios and the latest time steps. It does suggest however, that any high marsh in the Hudson River (such as Piermont Marsh) that converts to a regularly-flooded marsh may have higher resilience.

### 2.7. Other marsh accretion

Other wetland types can also gain elevation over time via vertical accretion mechanisms, though the model is less sensitive to these parameters. The inland-fresh marsh accretion rate was set to 1 mm/yr. Studies of fens and freshwater marshes in Michigan and Georgia suggest this as an appropriate estimate based on $^{210}$Pb measurements (Craft and Casey, 2000; Graham et al., 2005). Tidal fresh marsh accretion was set to a constant 5 mm/yr based on data presented by Neubauer et al. (2002). Accretion feedback was not considered due to a lack of site-specific data. Also lacking site-specific data, values of 1.6 mm/yr and 1.1 mm/yr were assigned for swamp and tidal swamp accretion, respectively which were measured in Georgia (Craft, 2012, 2008).

### 2.8. Beach sedimentation

Average beach sedimentation rates are assumed to be lower than marsh-accretion rates due to the lack of vegetation to trap suspended sediment, though it is known to be highly spatially variable. Lacking site specific information, beach sedimentation was set to 0.5 mm/yr, a commonly used value in SLAMM applications. It is worth noting that beach nourishment, predominant throughout the study area, is not accounted for in these SLAMM simulations, but different nourishment scenarios could be added to the model for future analyses.

### 2.9. Erosion rates

Erosion is another important process that may determine conversion of coastal areas to open water. Based on the analysis of Leatherman et al. (2000) who examined over 100 km of shoreline in Southern Long Island, long-term horizontal erosion rates of 0.44 m/yr. were applied to beach and tidal flats. Within SLAMM projections, the beach (or tidal flat) to open water interface is especially uncertain due to local variability in erosion and aggradation rates, wetlands and elevation data that are often not tidally coordinated, beach nourishment, and frequent waterline reformation due to storm events.

For marshes, erosion rates were set to 1 m/yr. (Fagherazzi, 2013). In SLAMM marsh erosion is modeled only at the marsh to open-water interface and erosion occurs only if there is adequate fetch (>9 km). For this reason, marshes in SLAMM have been shown to be considerably less sensitive to this parameter than accretion parameters (Chu-Agor et al., 2010).

### 2.10. Model calibration

SLAMM calibration was carried out by applying the initial-condition tides model to the study area but with no sea-level rise, accretion or erosion considered. With these “time-zero” projections, the consistency between elevation data, the current land coverage, modeled tidal ranges and hydraulic connectivity was assessed. Due to the lack of horizontal precision in land-cover data, elevation map uncertainty, and simplifications within the SLAMM conceptual model, some cells may be inundated too often with respect to the initial land cover identification (e.g. dry land that is inundated every day), and become converted to a different category. Where significant land-cover changes occur, additional investigation was required to confirm that the land cover of a particular area was correctly represented by time-zero results. For example, the high resolution elevation data allowed the identification of small channels in a several marsh areas not captured by the wetland layer. Otherwise, changes were reduced by calibrating tide ranges, within the variability reflected in the data, or by adding dikes or seawalls that were inadequately represented in our data sets (for example at LaGuardia Airport). Inundation-frequency maps were used to identify areas that should have been connected to tidal waters but had barriers in the digital elevation map that limited this connectivity. Consequently the DEM was further hydro-enforced where necessary.

### 2.11. Uncertainty setup

An important objective of this analysis was to study the confidence of the results with respect to input-data uncertainties. All of the site-specific data required by SLAMM, such as the spatial distribution of elevations, wetland coverages, tidal ranges, accretion and erosion rates, local sea-level rise and subsidence rates, may be affected by uncertainties that can propagate into the predicted outputs. For each of the model input parameters, an uncertainty distribution was derived based on available site-specific data. Distributions were selected to reflect measurement errors, uncertainty within measured central tendencies, and professional judgment (Firestone et al., 1997). Mechanistic considerations regarding the proper distribution type and the feasible bounds of the variable were considered.

Because SLAMM calculates equilibrium effects of SLR based on relatively large time-steps, long-term erosion rates, accretion rates, and SLR rates were used to drive model predictions. Therefore, the uncertainty distributions described in the following paragraphs are based on long-term measurements rather than incorporating short-term variability within measurements. Cell-by-cell spatial variability was considered for elevation data and VDATUM corrections, while the majority of the input parameters had uncertainty distributions that varied on a subsite basis. The distributions for SLR rate, long-term erosion rates, and accretion rates were applied uniformly throughout the study area.

One important limitation that has to be considered when interpreting these results is that the uncertainties of the general conceptual model in describing system behaviors (model framework uncertainty) are not taken into account. Within this uncertainty estimation, the flow chart of marsh succession is fixed. For example, low marshes must initially pass through a tidal flat category before becoming open water rather than directly converting to open water under any circumstance.

The distribution of possible SLR scenarios was derived from the recent NYC Panel on Climate Change Report (NPCC2) (Rosenzweig and Solecki, 2013) and the ClimAID report (Rosenzweig et al., 2011). The NPCC2 study estimates that by the 2050s the sea-level rise (with respect to 2000–2004 baseline level) at the Battery in NYC has a 10% probability to be 17.8 cm (7 in) or less, and a 90% probability to be less than or equal to 78.7 cm (31 in). From this information, SLR was extrapolated to 2100 and a triangular probability distribution, shown in Fig. 5, was considered for SLR by 2100 with a most likely SLR of 1.04 m (41 in). Based on professional judgment and additional literature estimates of eustatic SLR (Grinsted et al., 2009; Vermeer and Rahmstorf, 2009), we set the *minimum* SLR rate to 0.35 m by 2100 rather than using this as the 10th percentile. The highest possible SLR rate scenario was set to 2.35 m (92.5 in) by 2100.

Elevation-data uncertainty was evaluated by creating a new elevation map for each Monte Carlo iteration, by adding a spatially-autocorrelated error field to the existing digital elevation map (Darnell et al., 2008; Heuvelink, 1998; Hunter and Goodchild, 1997). This approach uses the normal distribution as specified by the Root Mean Squared Error (RMSE) for the LiDAR-derived dataset and applies it randomly over the entire study area, with spatial autocorrelation included (Hunter and Goodchild, 1997). It was assumed that elevation errors were strongly spatially autocorrelated, using a “p-value” of 0.2495, which results in tight clusters of similar data errors. The declared LiDAR RMSEs are: 9 cm for Hudson, Nassau and Suffolk Counties, and 12.5 cm for New York City.

Similarly, a vertical-datum-correction uncertainty was also applied via autocorrelated maps. The MTL to NAV88 transformation grids from NOAA covering the study area have a nominal maximum uncertainty that ranges between 9 cm and 11 cm. Because of the complicated boundaries of these datasets as compared to the study

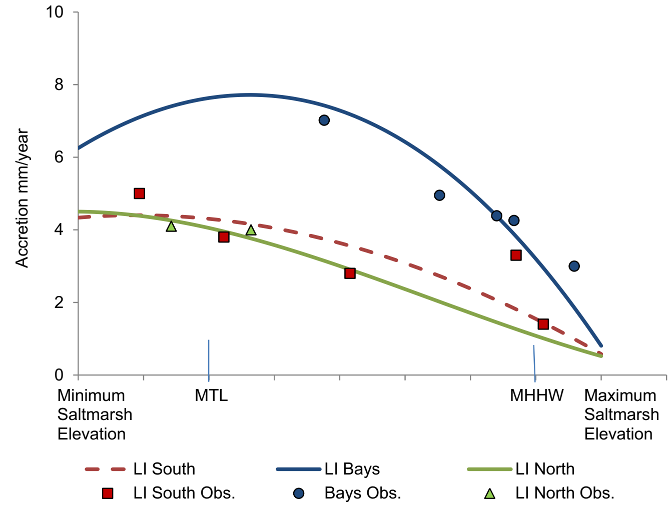


**Fig. 4.** Regularly-flooded marsh accretion models derived from MEM plotted against available data.

project boundaries and the similar maximum cumulative uncertainties of the datasets, the RMSE for the datum correction was set to 10 cm for the entire study area. Like the DEM uncertainty the assumption of strong spatial autocorrelation was maintained and a “p-value” of 0.2495 was applied.

For tide ranges, the uncertainties were modeled as normal distributions with standard deviations equal to the spatial variability observed in the subsite area when data were available. Standard deviations were widened conservatively when multiple measurements were not available. The “salt-elevation” uncertainty was derived by first estimating the salt elevation based on the tide range (selected from the tide-range distribution) using the relationship shown in Fig. 3. Then a further uncertainty multiplier was drawn reflecting the confidence intervals shown in Fig. 3 (the derived standard deviation for the salt elevation was 9 cm).

For all other input parameters, uncertainty distributions where derived from the literature when available or otherwise assigned as uniform distributions with wide uncertainty range. The overall characteristics of selected uncertainty distributions are summarized in Table 2 below.

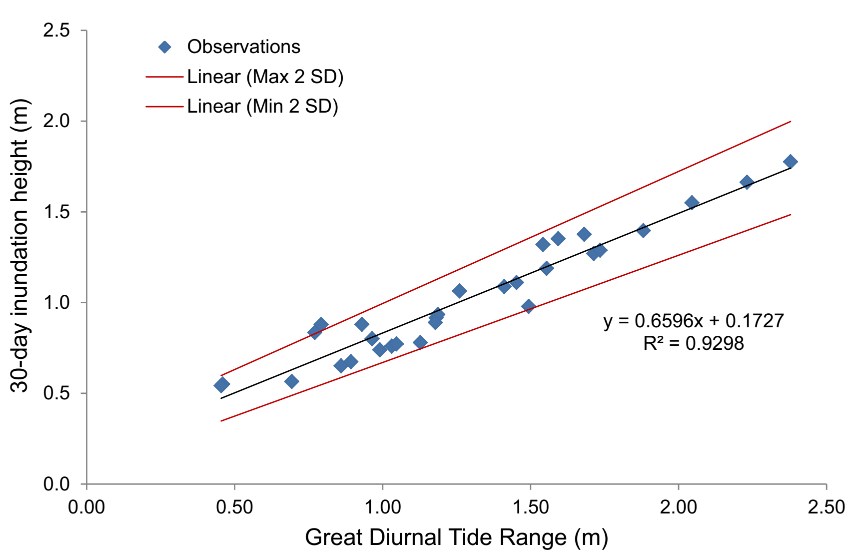


**Fig. 3.** Great diurnal tide range to 30-Day inundation height/salt elevation relationship derived from NOAA and long island shore data.

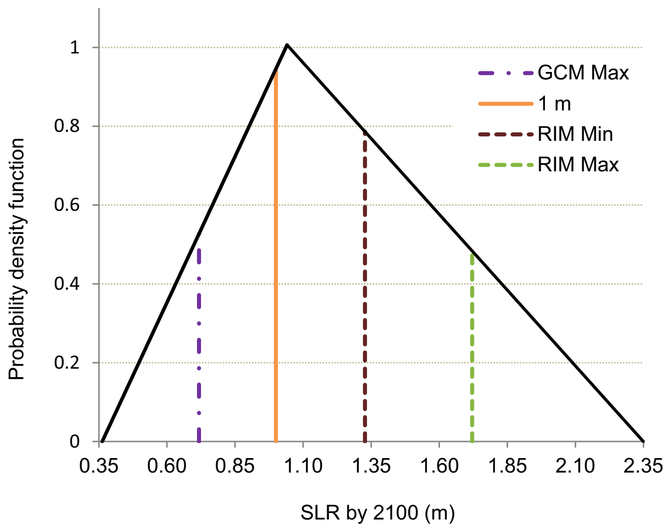


**Fig. 5.** SLR probability distribution used to drive uncertainty estimation (SLR_Uncertainty_Manuscript.xlsx).

A more complex set of distributions was required for IFM (high marsh) and low RFM (low marsh) for which mechanistic accretion models had been applied. For IFM the linear accretion-elevation relationship used in the deterministic model runs was maintained in the uncertainty estimation effort. The maximum and minimum accretion rates assigned at the boundaries of the marsh elevation range were drawn from probability distributions. Triangular distributions were used to draw both the minimum and maximum accretion values. The most likely probabilities were set to the maximum and minimum values used in the deterministic runs (4.23 mm/yr and 4.06 mm/yr, respectively). The range for these triangular distributions was estimated by adding two standard deviations to the most likely value or subtracting one standard deviation (to avoid negative accretion rates). The resulting range of maximum accretion rates was [2.38, 7.94] mm/yr., and for the minimum accretion rate it was [2.21, 5.91] mm/yr.

Similarly, the uncertainty in the accretion-feedback curves applied to low marshes was estimated by considering the uncertainty and variability within available accretion data. Accretion-measurement uncertainty and associated elevation-data uncertainty were either provided or estimated by considering the elevation variability around the sampling location (Fig. 6). For simplicity, only maximum and minimum accretion rates were considered as uncertainty variables. Given this choice, the calibrated MEM model identified for the deterministic runs (see Fig. 4) can be varied by these two rescaling factors. Interpreting Fig. 6, any accretion feedback curve drawn between these two red lines with the same general parabolic shape could be produced by one of the uncertainty model's iterations. A low minimum accretion rate could be paired with a high maximum accretion rate for example, providing a very strong feedback. The propagation of input-parameter uncertainty into model predictions cannot be analytically derived due to the non-linear spatiotemporal relationships that govern wetland conversion. Therefore, the SLAMM uncertainty estimation module employs a Monte Carlo approach in which the model is run hundreds of times over different input parameters simultaneously drawn from their uncertainty distributions using efficient Latin-Hypercube sampling. Results are then assembled into probability distributions of estimated land coverages. The number of model realizations ranged from 100 to 300, depending on the study area (Table 3) resulting in approximately 42,000 h of CPU time. The fewest runs were produced for Suffolk East as it had the longest CPU time per iteration. Extra runs were produced for the New York City study area to add precision to confidence intervals and to assess the effect of added iterations on uncertainty-map predictions as discussed below.

## 3. Results

A summary of overall land-cover changes for the entire study area is shown in Table 4. Of the tidal marshes, high marshes (irregularly-flooded marshes) are predicted to have the most vulnerability under all SLR scenarios with predicted losses ranging from over 3500 to over 8000 ha. In contrast, low marshes are predicted to make significant gains moving from 2200 ha of land coverage observed today to between 4200 and 7100 ha by 2100. In addition, from 1500 to 8600 ha of developed dry land and from 3700 to nearly 14,000 ha of undeveloped dry land are predicted to become flooded and convert to a different land type. Undeveloped dry lands convert to various wetland types depending on the frequency of flooding, while developed dry lands convert to “flooded developed dry land.” Open water is also predicted to expand by 3400 ha under the most conservative SLR scenario, and by more than 14,000 additional ha under RIM Max.

Another way to examine these results is to combine data for all tidal marshes (regularly-flooded marsh, irregularly-flooded marsh, tidal fresh marsh, and transitional salt marsh). Currently tidal marshes occupy nearly 12,000 ha throughout the study area. Under the GCM Max SLR scenario, total-marsh land cover is predicted reach 14,000 ha, a net gain of over 2000 ha. Looking at higher SLR scenarios, these gains are reduced to approximately 300 has.

**Table 2**
Summary of SLAMM input parameters uncertainty distributions.

| Parameter | Uncertainty distribution | Min | Max | Most likely | Units | Notes |
|---|---|---|---|---|---|---|
| Marsh erosion | Uniform | 0.0 | 2.0 | | m/yr. | Fagherazzi, 2013 |
| Swamp erosion | Normal | 0.2[a] | 1.8[b] | 1.0 | horz. m/yr. | Professional Judgment |
| Tidal flat erosion | Truncated Normal | 0.0 | 2.3[b] | 0.4 | horz. m/yr. | Leatherman et al., 2000<br>Wide range to account for storms and beach nourishment |
| Tidal fresh marsh accretion | Triangular | 2.0 | 18.0 | 5.0 | mm/yr. | Neubauer, 2008<br>Neubauer et al., 2002 |
| Inland fresh marsh accretion | Normal | 0.7[a] | 1.3[b] | 1.0 | mm/yr. | Craft and Casey, 2000<br>Craft and Richardson, 2008 |
| Tidal swamp accretion | Uniform | 0.6 | 2.8 | | mm/yr. | Craft, 2012<br>Data collected in Georgia |
| Swamps | Uniform | 0.2 | 3.4 | | mm/yr. | Craft, 2014<br>Data from Altamaha River, GA |
| Beach sedimentation | Uniform | 0.1 | 2.0 | | mm/yr. | Professional Judgment |

[a] 2.5th percentile.
[b] 97.5th percentile.

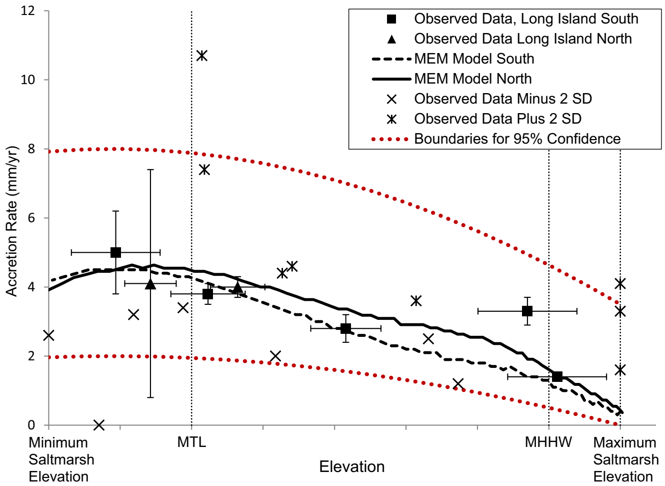


**Fig. 6.** Accretion modeling uncertainty investigation based on uncertainty and variability in observed data. Observed data are shown with one-standard-deviation error bars; Asterisks and "X" marks represent observed data with two standard deviations; the black line represents the best MEM fit used in deterministic runs; and, Dotted lines represent the 95% confidence interval assumed for the uncertainty estimation study.

**Table 3**
Uncertainty iterations by study area.

| Study area | Suffolk East | Suffolk West | Nassau | NYC | Hudson |
|---|---|---|---|---|---|
| Iterations run | 100 | 150 | 200 | 300 | 200 |

Nevertheless, the total-tidal marsh coverage area is predicted to be maintained even under the highest SLR scenario examined (RIM Max). From this point of view, coastal marshes of NY State appear to be somewhat resilient to SLR. However, as discussed further below, this result requires significant upland regions to be left undeveloped and made available for future marsh habitat.

Fig. 7 illustrates the predicted interplay between high marshes, low marshes and tidal flats at the end of the century. Under lower SLR scenarios, irregularly-flooded marshes are converted into regularly-flooded marshes, a habitat change that can have significant effects on marsh salinity and suitability of habitat for species that rely on these marshes. As predicted SLR exceeds 1 m, low marshes also are forecast to be lost and non-vegetated tidal flats increase.

The robustness of these model predictions has been investigated by an uncertainty estimation study. The New York City uncertainty results presented here are the result of 300 individual model predictions. Given the spatial complexity of this model, estimating prediction uncertainties was computationally intensive, with over 40,000 h of CPU time required to develop uncertainty results for the entire study area. Increasing the number of iterations to one or ten thousand was untenable. To account for this limitation, non-parametric statistical methods using the properties of binomial distributions were used to calculate the confidence of the percentiles accounting for the number of iterations (Walsh, 1962). The land-cover confidence intervals reported are the most conservative confidence boundaries of the percentiles (e.g. the 5th percentile curve is reported as its lowest 5% confidence boundary, and the 95th percentile curve by its highest 95% confidence boundary, shown as the bold lines in Fig. 8).

Fig. 8 also illustrates how the coverage of NYC coastal marshes evolves over time when considering all model uncertainties simultaneously. As expected, the confidence interval widens over time as several uncertainties become more prominent. While coastal marshes are predicted to increase overall, this graph does not account for changes in habitat towards more regularly-flooded and more saline wetlands. In addition, these model results must be interpreted as optimistic considering that all undeveloped dry land is assumed to be available for conversion to marsh habitats, no future development or sea-wall construction is assumed, and no marsh losses due to anthropogenic impacts (such as boat traffic or water pollution) are included.

Fig. 9 shows the same graphic but includes deterministic results for each of the four SLR scenarios within the confidence interval. From this graph it appears that the variable producing the most width in the predicted confidence intervals is the uncertainty in SLR scenarios as opposed to other input-parameter and data uncertainties.

To test this assertion, an additional uncertainty estimation study was run, keeping the "most-likely" SLR scenario fixed at 1.04 m and allowing all other model parameters and spatial data to be varied. Fig. 10 illustrates the results of these simulations. The confidence interval provided by the uncertainty results with SLR-fixed (dotted lines) is quite narrow compared to the confidence intervals when

**Table 4**
Land cover change predicted by 2100 compared to initial conditions. Negative change values indicate loss and positive show gains.

| Land cover category | Hectares in 2004 | Land cover change from 2004 to 2100 for different SLR scenarios (ha) | | | |
|---|---|---|---|---|---|
| | | GCM max | 1 m | RIM min | RIM max |
| Estuarine open water | 194,583 | 2770 | 5439 | 8295 | 12,777 |
| Open ocean | 153,573 | 632 | 802 | 1079 | 1450 |
| Undeveloped dry land | 126,390 | −3731 | −6505 | −9881 | −13,916 |
| Developed dry land | 82,942 | −1495 | −3112 | −5503 | −8637 |
| Irreg.-flooded marsh | 8401 | −3462 | −6781 | −7773 | −8069 |
| Swamp | 3456 | −207 | −373 | −543 | −710 |
| Inland open water | 2845 | −171 | −310 | −407 | −493 |
| Regularly-flooded marsh | 2216 | 4190 | 6962 | 7095 | 6165 |
| Ocean beach | 1840 | −251 | −127 | −29 | 65 |
| Estuarine beach | 1797 | −715 | −894 | −1049 | −1223 |
| Tidal flat | 1405 | −122 | 532 | 1734 | 2337 |
| Trans. salt marsh | 1187 | 1301 | 1676 | 2010 | 2259 |
| Inland-fresh marsh | 628 | −79 | −172 | −213 | −288 |
| Tidal swamp | 323 | −132 | −205 | −257 | −282 |
| Flooded developed dry land | 123 | 1495 | 3112 | 5503 | 8637 |
| Tidal-fresh marsh | 76 | −10 | −28 | −43 | −53 |
| Inland shore | 35 | 0 | 0 | 0 | 0 |
| Rocky intertidal | 17 | −12 | −14 | −15 | −16 |
| Riverine tidal | 5 | −2 | −2 | −2 | −2 |

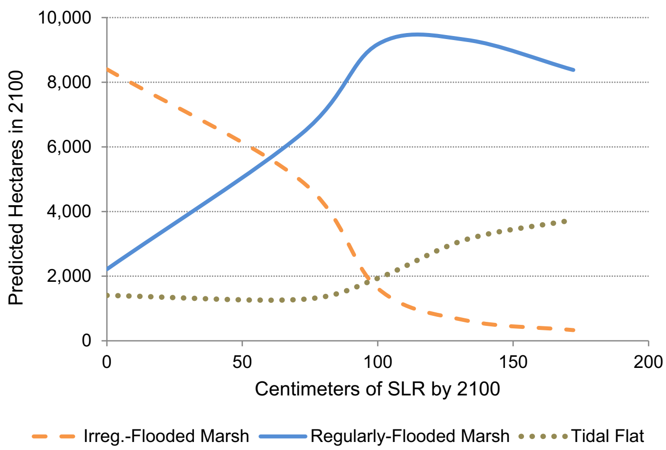


**Fig. 7.** Marsh and tidal-flat fate in the entire study area as a function of SLR by 2100.

SLR is also varied (solid black). This result is somewhat surprising given the wide variability introduced to accretion rates (Fig. 6) and the thorough accounting of spatial uncertainty in elevation and tide data. This result suggests that overall, if the future SLR scenario were to be known, SLAMM model results do not have a particularly wide confidence interval. However, this result does not include uncertainties raised by factors outside of the model domain, such as anthropogenic changes to the landscape, or uncertainties driven by the model structure itself.

Given the importance of upland-migration corridors, spatial analysis of model results is critical to better understand predicted marsh dynamics. In addition, SLR effects are predicted to be spatially variable across the study area with some areas at higher risk of marsh loss. Heavy marsh losses are predicted in vulnerable microtidal regimes behind the barrier islands south of Long Island and these barrier islands themselves are found to be subject to considerable dry-land losses. The vulnerability of low-tide-range wetlands to SLR has been widely reported in other studies and is documented in the literature (Kirwan et al., 2010). It can be simply explained if you consider that a larger tidal amplitude produces a wider range of elevations in which tidal marshes can exist.

While estimation of predition uncertainty has the potential to add complexity to a model simulation, it simultaneously can simplify results by reporting all possible SLR scenarios in a single probabilistic metric. Maps of uncertainty results can provide a spatial context to the stochastic simulations. Some examples of uncertainty maps derived for this project are: "Percent Likelihood of Habitat Change" (the likelihood that a cell has changed category – Fig. 11); "Probability that a cell is a coastal wetland" (includes all tidal marsh and beach categories – Fig. 12). Other maps not shown, but available throughout the study area on the project data repository website (http://www.warrenpinnacle.com/prof/SLAMM/NYSERDA/) include "Probability that a cell is flooded-developed

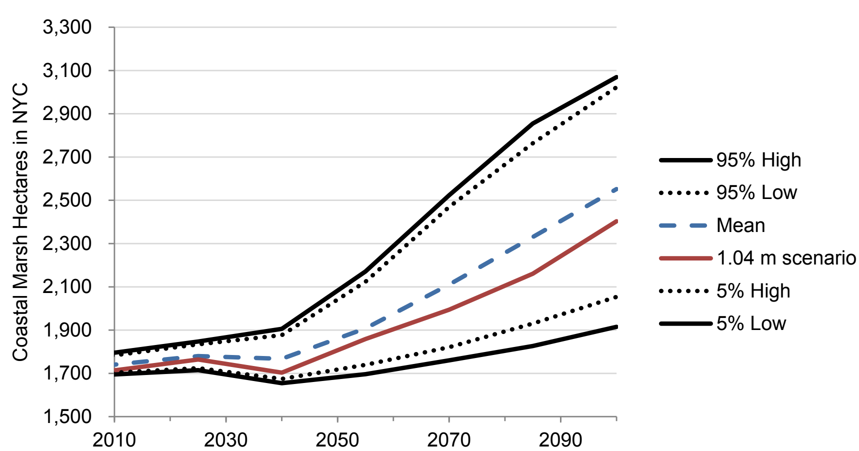


**Fig. 8.** Uncertainty results confidence intervals for coastal marshes in NYC.

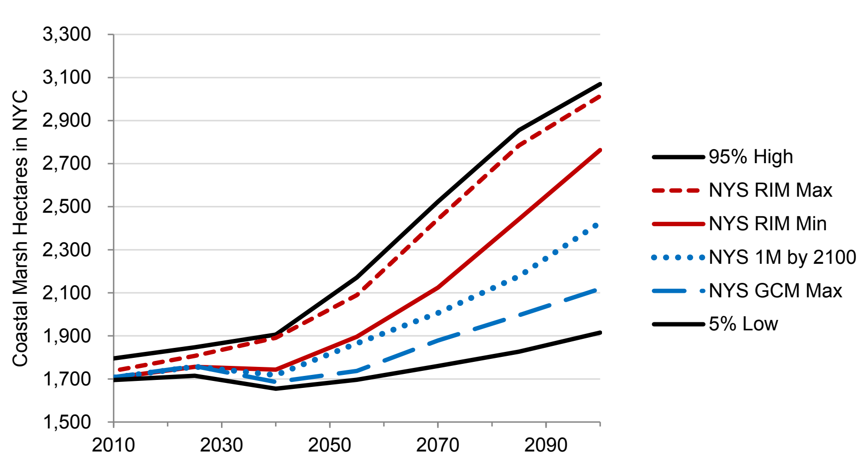


**Fig. 9.** Confidence interval for coastal marsh in black lines compared to deterministic estimates for the four SLR scenarios.

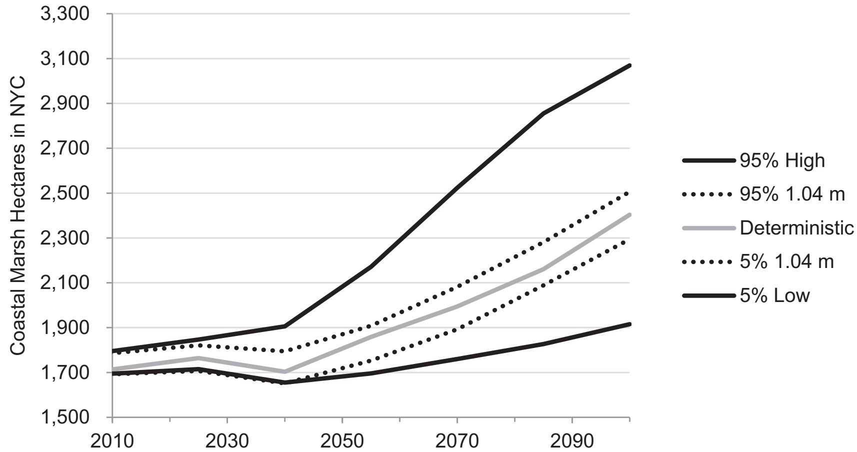


**Fig. 10.** Confidence interval when *all* input parameters are randomly sampled from their distributions (solid black lines) compared to the confidence interval when SLR scenario is set to 1.04 m by 2100 while all *other* parameters are randomly varied (dotted lines).

land"; and "Probability that a land category has converted to open water." These maps were derived for the years 2025, 2055, 2085, and 2100. Model results for New York City suggest moderate to high probabilities of habitat changes in both Jamaica Bay and northwestern Staten Island (Fig. 11), but also suggest moderate to high probabilities that these regions will include coastal wetlands in 2100 (Fig. 12).

## 4. Discussion

The Sea-Level Affecting Marshes Model (SLAMM) is a valuable tool to quantify the potential changes in marsh communities under the stress of accelerated SLR. Moreover, the stochastic uncertainty estimation module built in to SLAMM allows time series of deterministic model predictions to be presented with confidence intervals. Numerical results can be informative, but spatial analysis is

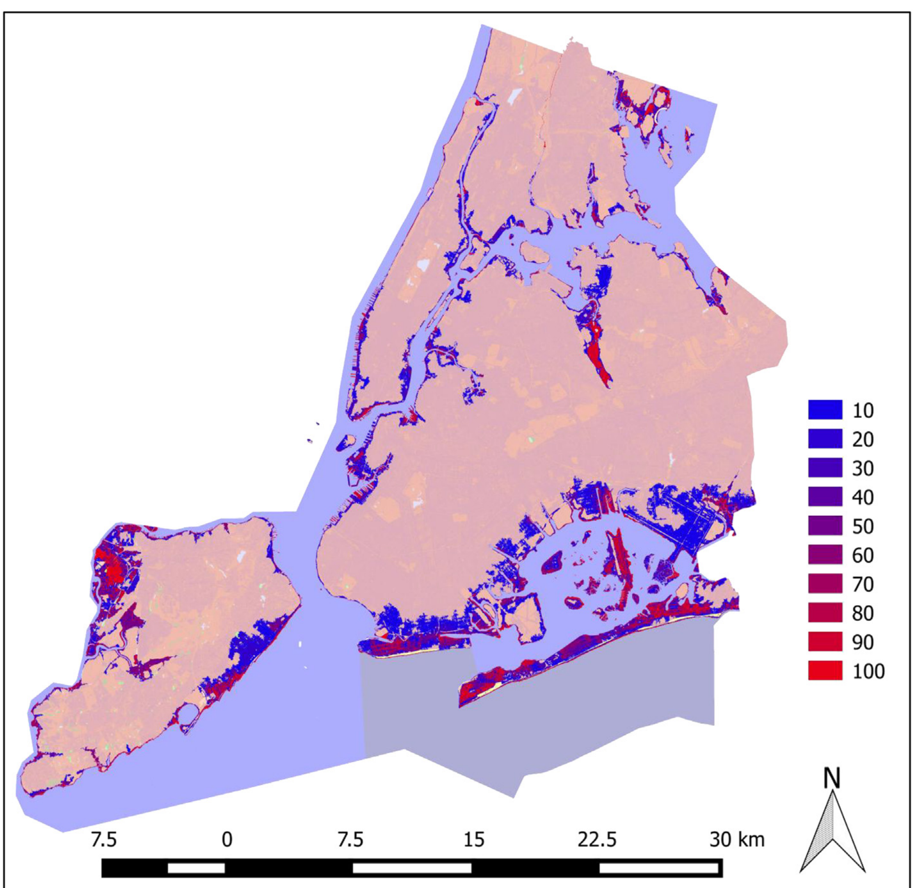


**Fig. 11.** NYC percent likelihood of habitat change by 2100.

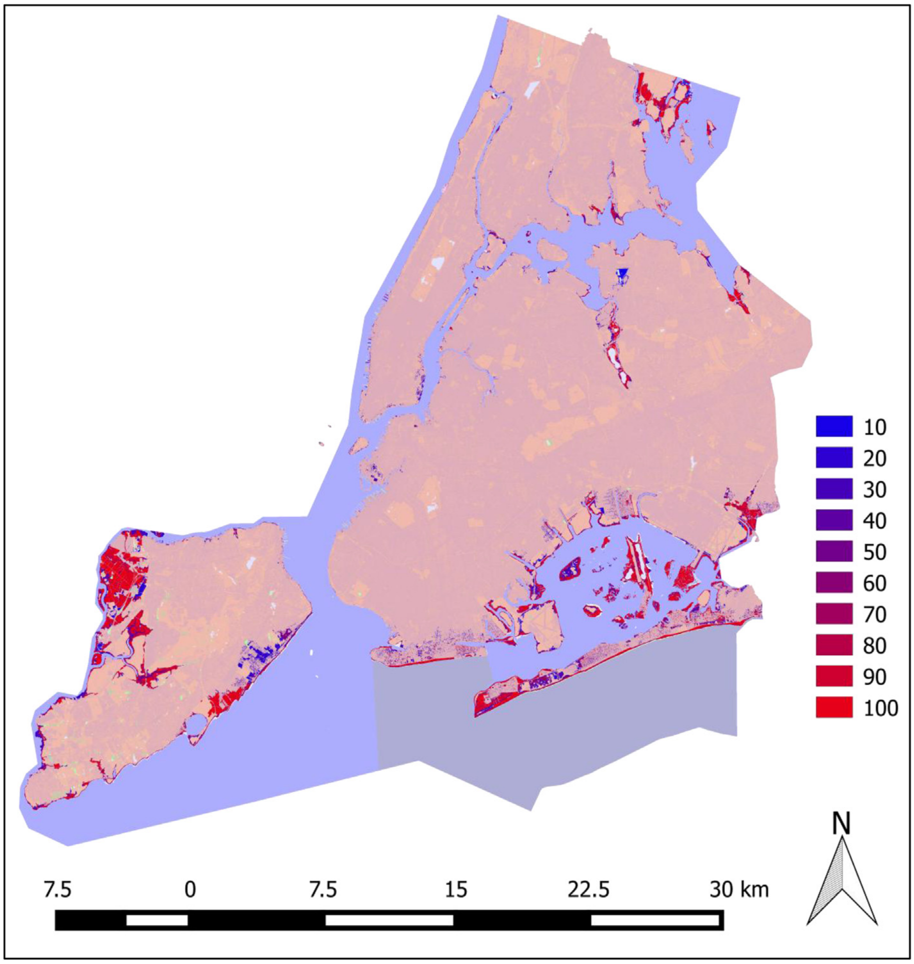


**Fig. 12.** NYC percent likelihood of coastal wetland in the year 2100.

indispensable in identifying areas where proper land use management could assist marsh maintenance and migration. An example analysis is shown below for Jamaica Bay in Fig. 13.

In Fig. 13, panel A shows the current tidal-wetland coverage while panels B and C show the predicted coverage at 2100 under 1 m and RIM Max scenarios respectively (open water and tidal flat are transparent with Google earth imagery beneath). One can observe that under 1 m of SLR most of the current area occupied by marshes today is still predicted to be marshlands in 2100. However, most of the existing high marshes (orange in panel A) are replaced by low marshes (light blue in panels B and C). Under a more aggressive SLR scenario (panel C), existing marshes are either predicted to be converted to low marshes or mostly replaced by tidal flats or open water (transparent). As is generally the case throughout the study area, total marsh land cover is not predicted to diminish because marshes are migrating inland to undeveloped dry lands. Panel D shows the 2004 land cover of areas that are predicted to be occupied by marshes at 2100 under RIM Max. The predominance of red suggests that the majority of these future marsh lands are currently dry lands. If these areas are properly managed, marshes could adapt to SLR by colonizing these areas. Finally, panels B and C also illustrate developed dry lands that are predicted to be regularly flooded by 2100 (in violet). These areas may be suitable for marsh migration in terms of flooding frequency. However, in order to make them functioning marsh-migration pathways several land use management actions would likely need to be taken, e.g. developed land re-appropriation. This example illustrates how spatial analysis of SLAMM projections can assist in identifying appropriate adaptation strategies.

Similar analyses can also support the identification of priorities in allocating available resources for managing current and future marsh areas. When considering the 1 m SLR scenario by 2100, resources could be split between protecting and maintaining the current marsh land cover and creating favorable conditions for marsh migration. For example, facilitating marsh accretion by restoring sediment sources and the deposition of dredged material may both prolong marsh viability and support marsh migration. On the other hand, when considering the RIM Max scenario, resources should be allocated towards creating migration pathways, as maintaining the current marsh areas is likely to become challenging. Additionally, spatial uncertainty maps can assist management decisions by explicitly accounting for uncertainty in the planning process. For example, an area that is highly likely to be open water in the future will need a different management than an area that is robustly predicted to be a marsh.

A major consideration in the examination of marsh migration pathways is anthropogenic changes to the landscape. Land that is currently considered undeveloped and available for future marsh colonization may become developed or protected by seawalls, creating hard barriers to marsh migration. It has been suggested that the fate of wetlands depends more on the human response to sea-level rise than the stress of sea level rise itself (Kirwan and Megonigal, 2013). The results of this SLAMM analysis are based on the current development footprint in coastal New York. Any

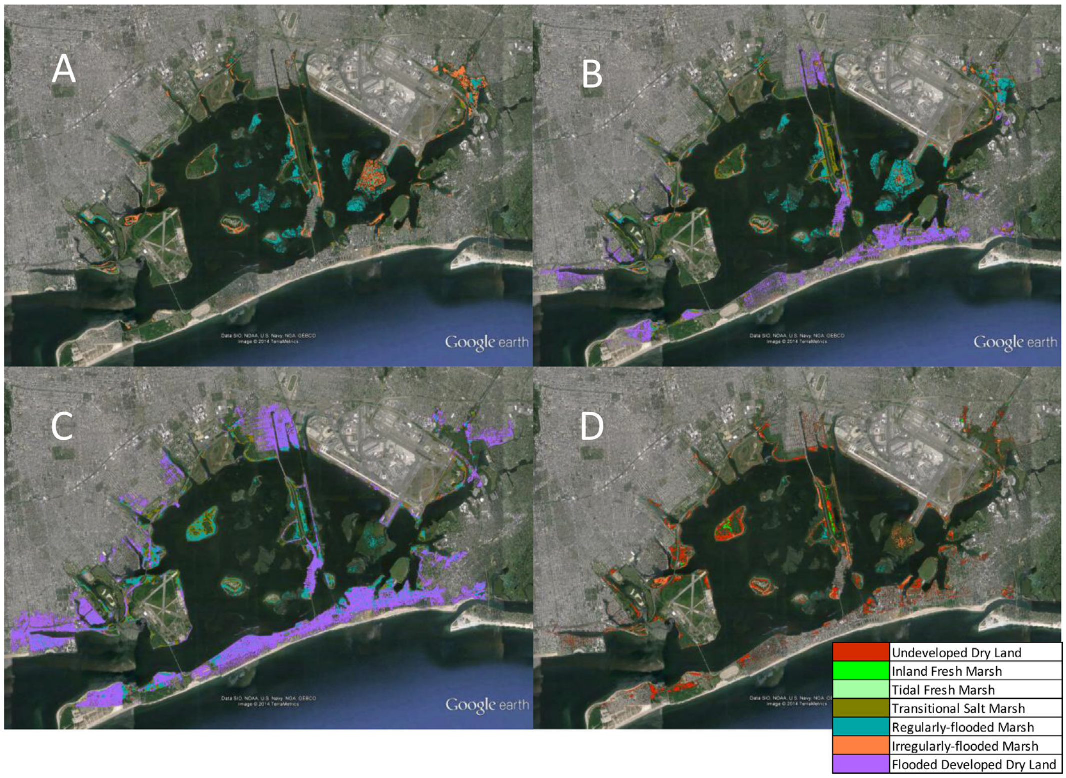


**Fig. 13.** Jamaica Bay projected tidal marsh dynamics. (A) Current coverage, (B) Predicted coverage by 2100 under 1 m SLR, (C) Predicted coverage by 2100 under RIM Max (1.7 m SLR), (D) Potential marsh migration areas.

future development in this region could affect the ability of coastal marshes to survive accelerated sea-level rise and would impact marsh ecosystem services such as carbon sequestration, animal habitat, recreation, and protection from storm surge.

## 5. Conclusions

This application of the SLAMM model utilizes a high horizontal resolution (5-m cells) and covers a large study area (all of coastal New York State). It incorporates the best-available elevation data, all existing tide data, and multiple land-cover data sets. This study combines these data with mechanistic marsh-accretion modeling to provide a thorough analysis of coastal-marsh fate across the study area. To address input-data and accretion-modeling uncertainties, a thorough estimation of prediction uncertainties was undertaken. Prediction results suggest that uncertainty over the rate and extent of future sea-level rise is by far the largest driver of uncertainty in model results.

There is another factor outside of the model domain that may be at least as important, however. This is uncertainty over how current undeveloped dry lands will be managed in the face of climate change impacts. Will lands be made available for marsh migration or will seawalls be aggressively built up to prevent transgression? Given the current model assumption that undeveloped dry lands are available for future marsh habitat, the model results presented herein must be seen as optimistic.

One other important potential for the model results shown here is that they can be used as a base analysis over which other analyses and data sets can be overlaid. For example, a simulation could be run with no dry-land migration, to look at a worst-case scenario for marsh migration corridors. Public-land to private land overlays could be incorporated or models of future development footprints to further refine model predictions in terms of anticipated anthropogenic actions. Roads data layers can be overlaid and this will characterize when these roads will be flooded and which roads are likely to prevent marsh habitat migration. Other anthropogenic effects may be built into the model such as effects from excessive nutrients, channel dredging, or erosion due to boat traffic.

Perhaps more importantly, the existing model results may be used by policymakers to prioritize restoration or management actions on existing wetlands or adjoining upland habitats. The results presented here should provide an important context for existing marsh restoration actions as well as habitat set asides for future coastal habitats.

## Acknowledgements

This project was funded by the New York State Energy Research and Development Authority through agreement number 28261. The opinions expressed in this report do not necessarily reflect those of NYSERDA or the State of New York, and reference to any specific product, service, process, or method does not constitute an implied or expressed recommendation or endorsement of it. We thank the Project Advisory Committee, which was instrumental in helping us incorporate the best input data available, providing insight into local wetland issues, and giving valuable feedback to improve the modeling process. We also extend our thanks to Benjamin Houston and Karen Kwasnowski at GroundPoint Technologies, LLC, for collecting the spatial data layers and completing the elevation layer hydrologic enforcement.

## Abbreviations

| | |
|---|---|
| CPU | Central Processing Unit |
| DEM | Digital Elevation Map |
| EPA | United States Environmental Protection Agency |

| | |
|---|---|
| GCM | General Climate Model |
| GIS | Geographic Information Systems |
| IFM | Irregularly-Flooded Marsh (High Marsh) |
| LiDAR | Light Detection and Ranging– method to produce elevation data |
| MEM | Marsh Equilibrium Model |
| MHHW | Mean Higher High Water (average highest tide each day) |
| MTL | Mean Tide Level |
| NAVD88 | North American Vertical Datum of 1988 |
| NOAA | United States National Oceanic and Atmospheric Administration |
| NWI | U.S. Fish and Wildlife Service's National Wetlands Inventory |
| NY | New York |
| NYC | New York City |
| NYS | New York State |
| NYSDEC | New York State Department of Environmental Conservation |
| NYCDPR | NYC Department of Parks and Recreation |
| NYSERDA | New York State Energy Research and Development Authority |
| PSU | Practical Salinity Units |
| RFM | Regularly-Flooded Marsh (Low Marsh) |
| RIM | Rapid Ice Melt |
| RMSE | Root Mean Standard Error |
| SLAMM | Sea-level Affecting Marshes Model |
| SLR | Sea-Level Rise |
| TSS | Total Suspended Solids |
| USACE | United States Army Corps of Engineers |
| VDATUM | NOAA Product for converting vertical datums |

## References


Anisfeld, S., 2014. Accretion Rates in Connecticut.
Armentano, T.V., Woodwell, G.M., 1975. Sedimentation rates in a Long Island marsh determined by 210Pb dating. Limnol. Oceanogr. 20, 452–456.
Chu-Agor, M.L., Munoz-Carpena, R., Kiker, G., Emanuelsson, A., Linkov, I., 2010. Global Sensitivity and Uncertainty Analysis of SLAMM for the Purpose of Habitat Vulnerability Assessment and Decision Making.
Clough, J., Park, Richard, Marco, P., Polaczyk, A., Fuller, R., 2012. SLAMM 6.2 Technical Documentation.
Cochran, J.K., Hirschberg, D.J., Wang, J., Dere, C., 1998. Atmospheric deposition of metals to coastal waters (Long Island Sound, New York USA): evidence from saltmarsh deposits. Estuar. Coast. Shelf Sci. 46, 503–522.
Craft, C., Clough, J., Ehman, J., Joye, S., Park, R., Pennings, S., Guo, H., Machmuller, M., 2008. Forecasting the effects of accelerated sea-level rise on tidal marsh ecosystem services. Front. Ecol. Environ. 7, 73–78.
Craft, C., 2008. Tidal Swamp Accretion.
Craft, C., 2012. Personal Communication.
Craft, C., 2014. Personal Communication – Swamp Accretion Rates.
Craft, C.B., Casey, W.P., 2000. Sediment and nutrient accumulation in floodplain and depressional freshwater wetlands of Georgia, USA. Wetlands 20, 323–332.
Craft, C.B., Richardson, C.J., 2008. Soil characteristics of the Everglades peatland. In: Everglades Experiments. Springer, pp. 59–72.
Dame, R.F., Kenny, P.D., 1986. Variability of Spartina alterniflora primary production in the euhaline North Inlet estuary. Mar. Ecol. Prog. Ser. 32, 71–80.
Darnell, A.R., Tate, N.J., Brunsdon, C., 2008. Improving user assessment of error implications in digital elevation models. Comput. Environ. Urban Syst. 32, 268–277. http://dx.doi.org/10.1016/j.compenvurbsys.2008.02.003.
Fagherazzi, S., 2013. The ephemeral life of a salt marsh. Geology 41, 943–944. http://dx.doi.org/10.1130/focus082013.1.
Firestone, M., Fenner-Crisp, P., Barry, T., Bennett, D., Chang, S., Callahan, M., Burke, A., Michaud, J., Olsen, M., Cirone, P., et al., 1997. Guiding Principles for Monte Carlo Analysis. Risk Assessment Forum. US Environmental Protection Agency.
Flessa, K.W., Constantine, K.J., Cushman, M.K., 1977. Sedimentation rates in a coastal marsh determined from historical records. Chesap. Sci. 18, 172–176.
Galbraith, H., Jones, R., Park, R., Clough, J., Herrod-Julius, S., Harrington, B., Page, G., 2002. Global climate change and sea level rise: potential losses of intertidal habitat for shorebirds. Waterbirds 25, 173. http://dx.doi.org/10.1675/1524-4695(2002)025[0173:GCCASL]2.0.CO;2.
Gesch, D.B., 2009. Analysis of lidar elevation data for improved identification and delineation of lands vulnerable to sea-level rise. J. Coast. Res. 49–58.
Geselbracht, L., Freeman, K., Kelly, E., Gordon, D.R., Putz, F.E., 2011. Retrospective and prospective model simulations of sea level rise impacts on Gulf of Mexico coastal marshes and forests in Waccasassa Bay, Florida. Clim. Change 107, 35–57.
Gilmer, B., Ferdaña, Z., 2012. Developing a framework for assessing coastal vulnerability to sea level rise in southern new England, USA. In: Otto-Zimmermann, K. (Ed.), Resilient Cities 2, Local Sustainability. Springer, Netherlands, pp. 25–36.
Glick, P., Clough, J., Polaczyk, A., Couvillion, B., Nunley, B., 2013. Potential effects of sea-level rise on coastal wetlands in Southeastern Louisiana. J. Coast. Res. 211–233. Understanding and Predicting Change in the Coastal Ecosystems of the Northern Gulf of Mexico Special Issue No. 63.
Graham, S.A., Craft, C.B., McCormick, P.V., Aldous, A., 2005. Forms and accumulation of soil P in natural and recently restored peatlands—Upper Klamath Lake, Oregon, USA. Wetlands 25, 594–606.
Grinsted, A., Moore, J.C., Jevrejeva, S., 2009. Reconstructing sea level from paleo and projected temperatures 200 to 2100 AD. Clim. Dyn. 34, 461–472. http://dx.doi.org/10.1007/s00382-008-0507-2.
Hagen, S.C., Morris, J.T., Bacopoulos, P., Weishampel, J.F., 2012. Sea-level rise impact on a salt marsh system of the lower st. johns river. J. Waterw. Port, Coast. Ocean Eng. 139, 118–125.
Haines, B.L., Dunn, E.L., 1976. Growth and resource allocation responses of Spartina alterniflora Loisel. to three levels of NH4-N, Fe, and NaCl in solution culture. Bot. Gaz. 224–230.
Hartig, E.K., Gornitz, V., Kolker, A., Mushacke, F., Fallon, D., 2002. Anthropogenic and climate-change impacts on salt marshes of Jamaica Bay, New York City. Wetlands 22, 71–89. http://dx.doi.org/10.1672/0277-5212(2002)022[0071:AACCIO]2.0.CO;2.
Heuvelink, G.B.M., 1998. Error Propagation in Environmental Modelling with GIS. CRC Press.
Hunter, G.J., Goodchild, M.F., 1997. Modeling the uncertainty of slope and aspect estimates derived from spatial databases. Geogr. Anal. 29, 35–49.
Kirwan, M.L., Guntenspergen, G.R., D'Alpaos, A., Morris, J.T., Mudd, S.M., Temmerman, S., 2010. Limits on the adaptability of coastal marshes to rising sea level. Geophys. Res. Lett. 37.
Kirwan, M.L., Megonigal, J.P., 2013. Tidal wetland stability in the face of human impacts and sea-level rise. Nature 504, 53–60.
Kolker, A.S., 2005. The Impacts of Climate Variability and Anthropogenic Activities on Salt Marsh Accretion and Loss on Long Island [WWW Document].
Leatherman, S.P., Zhang, K., Douglas, B.C., 2000. Sea level rise shown to drive coastal erosion. Eos, Trans. Am. Geophys. Union 81, 55–57.
Lee, J.K., Park, R.A., Mausel, P.W., 1992. Application of geoprocessing and simulation modeling to estimate impacts of sea level rise on the northeast coast of Florida. Photogrammetric Eng. Remote Sens. 58, 1579–1586.
Lee, J.K., Park, R.A., Mausel, P.W., Howe, R.C., 1991. GIS-related modeling of impacts of sea level rise on coastal areas. In: GIS/LIS'91 Conference, pp. 356–367.
Linthurst, R.A., Blum, U., 1981. Growth modifications of Spartina alterniflora Loisel. by the interaction of pH and salinity under controlled conditions. J. Exp. Mar. Biol. Ecol. 55, 207–218.
Linthurst, R.A., Seneca, E.D., 1981. Aeration, nitrogen and salinity as determinants of Spartina alterniflora Loisel. growth response. Estuaries 4, 53–63.
Maher, N.P., 2013. Accretion Collection Data for Long Island.
Mcleod, E., Poulter, B., Hinkel, J., Reyes, E., Salm, R., 2010. Sea-level rise impact models and environmental conservation: a review of models and their applications. Ocean Coast. Manag. 53, 507–517. http://dx.doi.org/10.1016/j.ocecoaman.2010.06.009.
Mendelssohn, I.A., Marcellus, K.L., 1976. Angiosperm production of three Virginia marshes in various salinity and soil nutrient regimes. Chesap. Sci. 17, 15–23.
Morris, J.T., Sundareshwar, P.V., Nietch, C.T., Kjerfve, B., Cahoon, D.R., 2002. Responses of coastal wetlands to rising sea level. Ecology 83, 2869–2877.
National Ocean Service, 2010. Tide Tables 2011 – East Coast of North and South America Including Greenland. US Department of Commerce, Silver Spring, MD.
National Ocean Service, 2013. VDatum: NOAA/NOS/Vertical Datum Transformation [WWW Document]. US Department of Commerce, National Oceanic and Atmospheric Administration. http://vdatum.noaa.gov/ (accessed 11.25.13.).
Neubauer, S.C., 2008. Contributions of mineral and organic components to tidal freshwater marsh accretion. Estuar. Coast. Shelf Sci. 78, 78–88.
Neubauer, S.C., Anderson, I.C., Constantine, J.A., Kuehl, S.A., 2002. Sediment deposition and accretion in a mid-atlantic (U.S.A.) tidal freshwater marsh. Estuar. Coast. Shelf Sci. 54, 713–727. http://dx.doi.org/10.1006/ecss.2001.0854.
Park, R.A., Lee, J.K., Mausel, P.W., Howe, R.C., 1991. Using remote sensing for modeling the impacts of sea level rise. World Resour. Rev. 3, 184–220.
Park, R.A., Trehan, M.S., Mausel, P.W., Howe, R.C., 1989. The Effects of Sea Level Rise on U.S. Coastal Wetlands, in: the Potential Effects of Global Climate Change on the United States: Appendix B – Sea Level Rise. U.S. Environmental Protection Agency, Washington, DC, pp. 1–1 to 1–55.
Pierson, N., 2013. Suffolk County Marine Water Quality Monitoring Data.
Reed, D.J., 1995. The response of coastal marshes to sea-level rise: survival or submergence? Earth Surf. Process. Landforms 20, 39–48. http://dx.doi.org/10.1002/esp.3290200105.
Rosenzweig, C., Solecki, W., DeGaetano, A., O'Grady, M., Hassol, S., Grabhorn, P., 2011. Responding to Climate Change in New York State: the ClimAID Integrated Assessment for Effective Climate Change Adaptation in New York State (No. 11–18). New York State Energy Research and Development Authority (NYSERDA), Albany, New York.
Rosenzweig, Solecki, 2013. New York City Panel on Climate Change, 2013: Climate Risk Information 2013: Observations, Climate Change Projections, and Maps.

Prepared for use by the City of New York Special Initiative on Rebuilding and Resiliancy, New York. Mayor's Office of Long-Term Planning & Sustainability, New York.
Schile, L.M., Callaway, J.C., Morris, J.T., Stralberg, D., Parker, V.T., Kelly, M., 2014. Modeling tidal marsh distribution with sea-level rise: evaluating the role of vegetation, sediment, and upland habitat in marsh resiliency. PLoS One 9, e88760.
Schmid, K., Hadley, B., Waters, K., 2014. Mapping and portraying inundation uncertainty of bathtub-type models. J. Coast. Res. 548–561. http://dx.doi.org/10.2112/JCOASTRES-D-13-00118.1.
Vasquez, E.A., Glenn, E.P., Guntenspergen, G.R., Brown, J.J., Nelson, S.G., 2006. Salt tolerance and osmotic adjustment of Spartina alterniflora (Poaceae) and the invasive M haplotype of Phragmites australis (Poaceae) along a salinity gradient. Am. J. Bot. 93, 1784–1790.
Vermeer, M., Rahmstorf, S., 2009. Global sea level linked to global temperature. Proc. Natl. Acad. Sci. 106, 21527.
Walsh, J.E., 1962. Handbook of Nonparametric Statistics. Van Nostrand Reinhold, New York.
Wilson, T., 2013. LIShore [WWW Document]. http://www.lishore.org/ (accessed 2.15.13.).
Woodruff, J.D., Geyer, W.R., Sommerfield, C.K., Driscoll, N.W., 2001. Seasonal variation of sediment deposition in the Hudson River estuary. Mar. Geol. 179, 105–119.
Wu, W., Yeager, K.M., Peterson, M.S., Fulford, R.S., 2015. Neutral models as a way to evaluate the sea level affecting marshes model (SLAMM). Ecol. Model. 303, 55–69. http://dx.doi.org/10.1016/j.ecolmodel.2015.02.008.
Zedler, J.B., 1980. Algal mat productivity: comparisons in a salt marsh. Estuaries 3, 122–131.